Int. J. Pharm. Investigation, 2026; 16(1):133-142.
https://www.jpionline.org

Original Article

In silico and *in vitro* Evaluation of Phytoconstituents for their NADPH Oxidase 5 (NOX5) Inhibitory Activity

Payal Shah[1,2], Gaurang Shah[2,*]

[1]Research Scholar, Gujarat Technological University, Ahmedabad, Gujarat, INDIA.
[2]Department of Pharmacology, L. M. College of Pharmacy, Navrangpura, Ahmedabad, Gujarat, INDIA.

ABSTRACT

Background: Reactive oxygen species (ROS), produced by different enzymes, play a role in oxidative stress, which is linked to the development of many diseases. The NADPH oxidase (NOX) enzyme family serves as a primary source of ROS, with NOX5 being a comparatively underexplored member regarding antioxidant activity and therapeutic targeting. **Materials and Methods:** A computational screening method was utilized to discover selective NOX5 inhibitors from a collection of phytochemicals. Promising compounds found via computational docking were subsequently evaluated for their capacity to inhibit ROS production using in-vitro tests, such as Nitroblue Tetrazolium (NBT) and cytochrome C reductase assays. **Results:** Multiple phytochemicals—Tanshinone IIa, Quercetin, Curcuminoids, Berberine, and Resveratrol-showed significant NOX5 inhibitory effects. These compounds demonstrated advantageous pharmacokinetic characteristics and drug-likeness attributes, suggesting their promise as therapeutic options. **Conclusion:** This research discovers natural substances with potential NOX5 inhibitory effects and favourable drug-like properties, indicating their promise as antioxidant agents for treating ROS-related conditions.

Keywords: NOX5, Docking, MD simulations, NBT assay, Cytochrome C reductase assay.

Correspondence:
Dr. Gaurang Shah
Department of Pharmacology, L. M. College of Pharmacy, Navrangpura, Ahmedabad 380009, Gujarat, INDIA.
Email: gaurang.shah@lmcp.ac.in

Received: 08-05-2025;
Revised: 14-07-2025;
Accepted: 26-09-2025.

INTRODUCTION

Oxidative stress caused due to imbalance between ROS production in cells and the ability of body to detoxify these reactive products, which results into accumulation of reactive free radicals in the body. These ROS reacts with various biochemicals in the body to oxidise them. Such oxidative products are responsible for various abnormalities such as cancer, cardiovascular, neurological, respiratory, inflammatory, renal, and sexual disorders (Pizzino *et al*., 2017).

Various enzymes within the body can generate ROS, including cytochrome P450 oxidases, monoamine oxidases, NADPH oxidases (the catalytic subunit of NADPH oxidases [NOX]), lipoxygenases, xanthine oxidase, uncoupled Nitric Oxide Synthase (NOS), and the electron transport chain in mitochondria. The majority of these enzymes generate ROS following their damage from ROS. In contrast, the primary function of NADPH oxidases is to produce ROS. They are generally located in various types of tissues. Consequently, NADPH oxidases are regarded as key targets for addressing these conditions (Vermot *et al*., 2021).

DOI: 10.5530/ijpi.20260444

There are various enzyme isoforms in the NOX enzyme family such as NOX1 to NOX7, DUOX1 and DUOX2 (Altenhöfer *et al*., 2015). NOX5 is absent in animal models such as mice and rats. Therefore, its function is not as clearly outlined as other NOX forms. KO strategies for bigger animals, such as rabbits, have recently become accessible but come with a high price tag. Therefore, utilizing specific NOX5 inhibitors could offer a more favourable method to investigate its impact in bigger animals. Limited information on NOX5 prevents considering it as a viable therapeutic target for any disease (Bedard *et al*., 2012).

In this study, we have screened several phytoconstituents identified from literature review using *in silico* processes like molecular docking, ADMET study and MD simulations to evaluate their antioxidant activity selectively against NOX5 enzyme. As, it has been reported that PC3 cell line express NOX5 enzyme (AGNES *et al*., 2009), we incorporated hit molecules obtained through *in silico* study, into *in vitro* study using NBT (Hyung *et al*., 2006) and cytochrome C reductase assay (Almeida *et al*., 2010) on PC3 cell line.

MATERIALS AND METHODS

Data assortment and processing

A total of 140 phytochemicals exhibiting recognized antioxidant properties were identified through comprehensive literature

review and their three-dimensional structures were sourced from PubChem (*PubChem*, n.d.). OpenBabel software was used to process the ligand molecules and convert them to PDBQT format for further molecular modelling process (O'Boyle *et al*., 2011).

Three dimensional crystal structure of dehydrogenase domain of the NOX5 protein having 2.20 A˚ resolution evaluated through X-ray diffraction (PDB ID: 5O0X) (Magnani *et al*., 2017) was got from RCSB PDB (protein data bank) (Protein Data Bank, n.d.). The receptor protein was pre-processed using AutoDock Vina (Morris *et al*., 2009; Steffen *et al*., 2010). To achieve balance in the protein's polarity and charges, polar hydrogens and Kollman charges were added and water molecules were removed. A receptor grid box was created having x, y and z co-ordinates 76×76×84 Aº, respectively. Co-ordinates for size and centres were set 67.516×4.006×68.476 Aº for x, y, and z dimensions, respectively. This protein structure was kept in PDBQT file to use it in molecular docking.

Molecular Docking

The ligand molecules were positioned on the NOX5 protein (5O0X) with AutoDock Vina for assessing the binding strength and interactions, resulting in ten poses for each ligand. The interactions between receptor protein and ligand were analysed using Biovia Discovery studio 2020 (Dassault Systèmes BIOVIA, Discovery Studio Modeling Environment, Release 2021, San Diego: Dassault Systèmes, 2020., n.d.) and hits were choosen having binding energy below -8.0 kCal/Mol. Being a known and previously reported NOX inhibitor, Apocynin was selected as a control to compare binding affinity of other compounds (Abliz *et al*., 2016; Cipriano *et al*., 2023; Tiwari *et al*., 2023).

ADMET Analysis

The lipinski's rule of 5 evaluates physicochemical properties like hydrogen bond donors and acceptors, molecular mass, oil to water partition coefficient, and rotational bonds of phytochemicals using virtual tools like SwissADME (Daina *et al*., 2017) and pkCSM (Pires *et al*., 2015; pkCSM: Pharmacokinetic properties, n.d.). Different drug likeliness rules such as Egan's rule, Ghose rule, Lipinski's rule of five, Muegge's rule and Veber's rule were also utilized on the chosen compounds with the help of SwissADME software to confirm their drug likeliness. The number of parameters that were violated in relation to these rules were also considered. Moreover, the pkCSM program was utilized to examine diverse ADMET attributes that aid in forecasting the pharmacokinetics of compounds, including traits like molar refractivity, water solubility, $CaCO_2$ cell permeability, topological polar surface area, intestinal absorption, unbound fraction, volume of distribution, renal clearance, liver toxicity, and the capacity to inhibit P-glycoprotein.

MD Simulations

Being a compound with the best binding affinity among all the compounds, Tanshinone IIa was incorporated to MD simulation through GROMACS (GROningen MAchine for Chemical Simulations) 2020.1 software (Abraham *et al*., 2015; M.J. Abraham, Berk Hess, E. Lindahl, n.d.) to evaluate its stability after binding with 5O0X. Chemistry at Harvard Macromolecular Mechanics (CHARMM36) force field (Huang *et al*., 2017) and CGenFF (CHARMM General Force Field) server were utilised for the generation of topology parameters of ligand molecule (Vanommeslaeghe K, Acharya C, Kundu S, Zhong S, Shim J, Darian E, Guvench O, Lopes P, Vorobyov I, 2009; Yu *et al*., 2012). Further, solvation with TIP3P water model along with the neutralization using Na+ and Cl– ions were carried out. Systems were equilibrated using NVT [number of particles (N), system volume (V) and temperature (T), (canonical) and NPT [number of particles (N), system pressure (P) and temperature (T), (isobaric-isothermic) ensemble for 100 pico seconds, and the final molecular dynamics run for 50 nano seconds was achieved for 5O0X-Tanshinone IIA complex. Plots of RMSD (ligand and protein), RoG (complex), SASA (complex) and Hydrogen bonds were plotted against time in ns along with the RMSF of complex against atoms.

NBT Assay

NBT absorbance assay was performed to measure intracellular superoxide generation (Whitehouse *et al*., 2016). PC3 cell line was obtained from the NCCS, Pune, India. Cells were pelleted and suspended in 1 mL PBS having pH 7.4. In 0.5 mL Eppendorf, 50 Ml of cell suspension was incubated for 10 min with 20 µL of different concentrations (25 µg/mL, 12.5 µg/mL, 6.25 µg/mL, 3.125 µg/mL and 1.56 µg/mL) of selected phytoconstituents prepared in 1% DMSO. 30 µL fMLF (1 mM) was added to activate NOX enzyme followed by the addition of 30 µL NBT (1 mg/mL) and 30 µL NADPH (200 µg/mL, prepared in PBS having pH 8). The reaction tubes were kept at 37ºC for the period of 3 min followed by the centrifugation at 13,300 rpm for 2 min at 4ºC temperature. Pellet was washed with 100 µL PBS and centrifuged at same condition. 100 µL Methanol was added to the reaction and centrifuged again at same condition. 50 µL of supernatant were taken in 96 well plate and reacted 50 µL KOH (2M) and 100 µL DMSO (99%). After 5 min of incubation, absorbance was measured at 610 nm against the control with no treatment and % inhibition of NOX enzyme was calculated at different concentrations of all phytoconstituents.

Cytochrome C reductase Assay

PC3 cells were pelleted and suspended in 1 mL PBS having pH 7.4. followed by the addition of 30 µL SLS (1%). Cells were centrifuged at 13,300 rpm for 5 min at 4ºC temperature and 30 µL supernatant was taken into 96 well plate. 20 µL of phytoconstituents having concentrations mentioned in NBT assay were added to the well.

Further, 30 µL fMLF (1 mM), 50 µL cytochrome C (4 mg/mL) and 30 µL NADPH (100 µg/mL) were added and absorbance at 550 nm was taken in kinetic mode up to 10 min against the well without drug treatment as a control and % reduction of cytochrome C was calculated.

RESULTS

Data assortment and processing

Magnani and colleagues used X-ray diffraction to reveal crystal structure and atomic model of the dehydrogenase domain of NADPH-Oxidase 5 (NOX5) (Magnani *et al.*, 2017). They provided a detailed description of the crystal structures for the catalytic FAD (flavin adenine dinucleotide) and heme-binding domains of NOX5. The complete three-dimensional configuration of essential interactions is described among the intracellular loops located within NADPH-oxidizing dehydrogenase domain and transmembrane domain. The C terminus works as a switch, regulating the enzyme's interaction with the NADPH substrate. The regulatory signals govern the conformational opening and closing of NADPH binding, functioning to activate or deactivate the initial stage of the redox reaction cascade. Consequently, we selected this design as our primary focus, providing a framework for identifying drugs that target NOX5 and interfere with ROS signaling

Molecular docking

The prepared PDBQT of 5O0X was used for molecular docking with optimized structures of 140 natural compounds. Docking was performed on the active site at which grid box was generated. Binding energy of all the compounds were observed and compounds having energy less than -8.0 Kcal/mol were described in the Table 1 along with 2D structures. Apocynin as a reported and known NOX inhibitor, observed with binding energy -6.7 Kcal/mol.

Various interactions were analysed between the phytoconstituents and amino acids present in active site (Figures 1 and 2). Tanshinone IIa with the highest binding energy (-11.9 Kcal/mol) found to interact by hydrogen bonding with amino acid Thr462. It also formed pi bonds with Trp695 and Phe461 and alkyl bonds with Pro460, Tyr 445, Phe447 and Ile538 (Figure 1A). Similarly, Ellagic acid interacted with Arg478 and Thr462 through hydrogen bonds, with Ile538 and Pro460 through pi-pi interactions and with Phe461 through pi-sigma interaction (Figure 1B). Emodin formed hydrogen bonds with Thr462 and Arg478, pi bonds with Trp695 and Phe461, along with the alkyl bonds with Ile538 and Pro460 (Figure 1C). Three hydrogen bonds (Arg478, His476, Thr462), three pi interactions (Tyr445, Phe461, Trp695) and one alkyl bond (Pro460) were observed in

Table 1: Compounds with binding energy less than -8.0 Kcal/mol and their 2D structures.

Molecule No.	Compound	2D structure	Binding Energy (Kcal/mol)
1	Tanshinone IIa	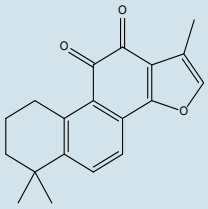	-11.9
2	Ellagic acid	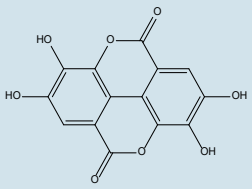	-10.8
3	Emodin	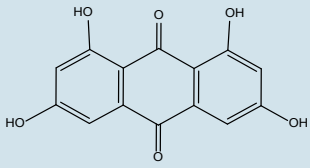	-10.7
4	Quercetin	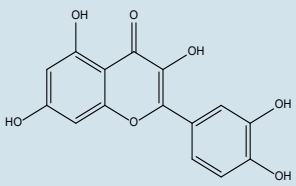	-9.7

Molecule No.	Compound	2D structure	Binding Energy (Kcal/mol)
5	Apigenin	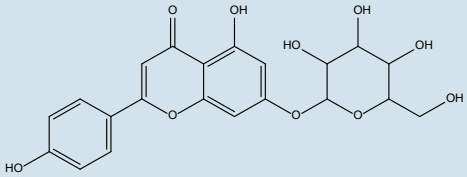	-9.6
6	Curcuminoid	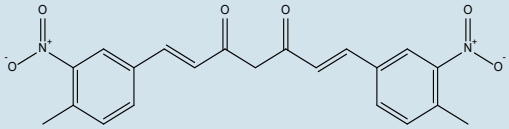	-9.5
7	Plumbagin	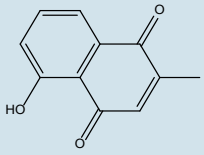	-9.1
8	Naringenin	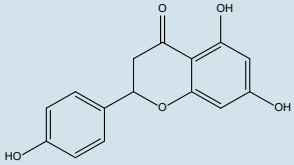	-8.5
9	Berberine	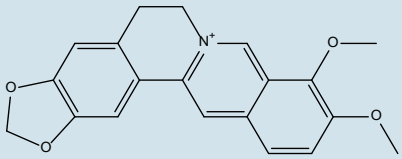	-8.4
10	Epigallocatechin	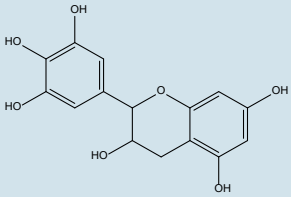	-8.3
11	Resveratrol	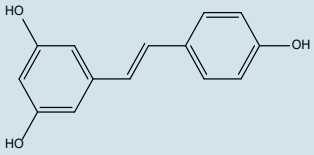	-8.2
12	Apocynin	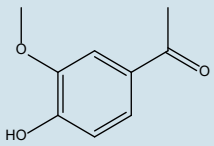	-6.7

the case of quercetin (Figure 1D). Apigenin formed hydrogen bonds with His459 and Thr462, pi-sigma bond (Phe461), alkyl bond (Pro460) and pi bond (Trp695) (Figure 1E). Curcuminoid interected through hydrogn bonding with Thr462 and Trp695, through pi interactions with Phe461 and Tyr445, through alkyl bond with Ile538 (Figure 1F).

Hydrogen bond with Thr462, alkyl bonds with Pro460 and Ile538, pi bonds with Phe461 and Trp695 were observed to be formed by Plumbagin (Figure 2A). Naringenin was found to form hydrogen bond with Arg478, pi bonds with Trp695 and Phe461, along with the alkyl bond with Val480 (Figure 2B). Berberine interacted with hydrogen bond (His476), pi bonds (Trp695, Phe461) and alkyl bonds (Pro460, Tyr445, Ile538, Arg478) as presented in Figure 2C. Epigallocatechin formed pi bonds with Phe461, Trp695,

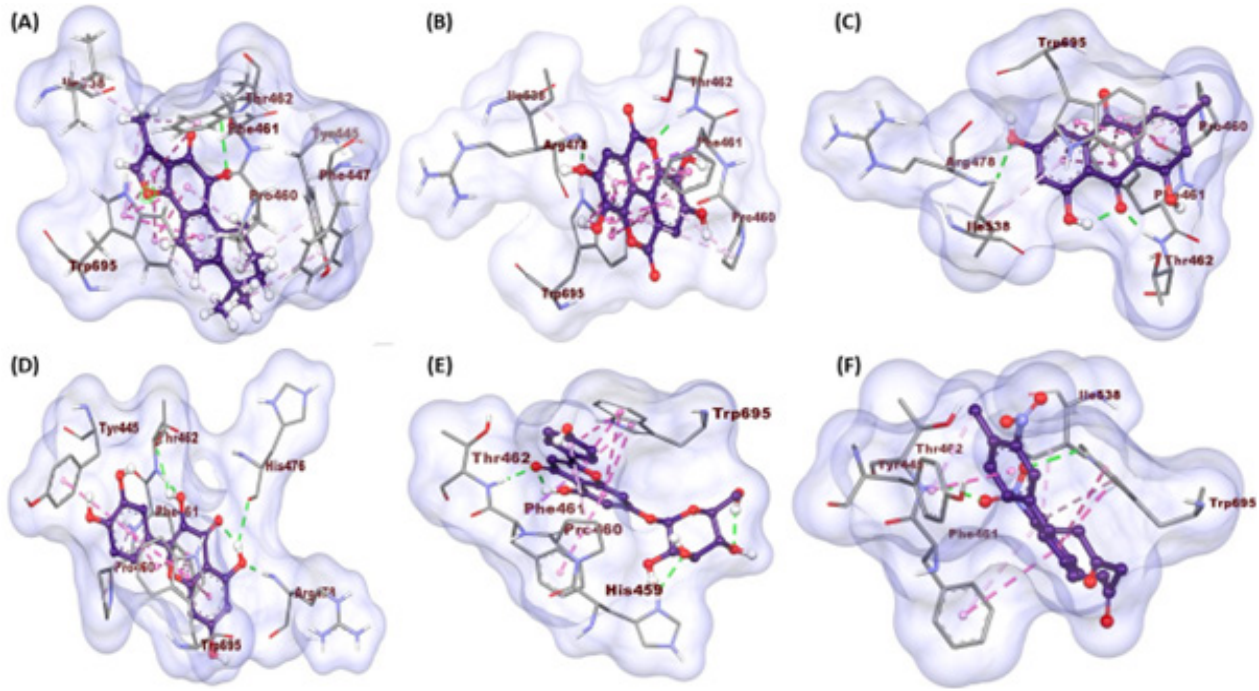

Figure 1: 3D poses and binding interactions of (A) Tanshinone IIa, (B) Ellagic acid, (C) Emodin, (D) Quercetin, (E) Apigenin and (F) Curcuminoid with 5O0X.

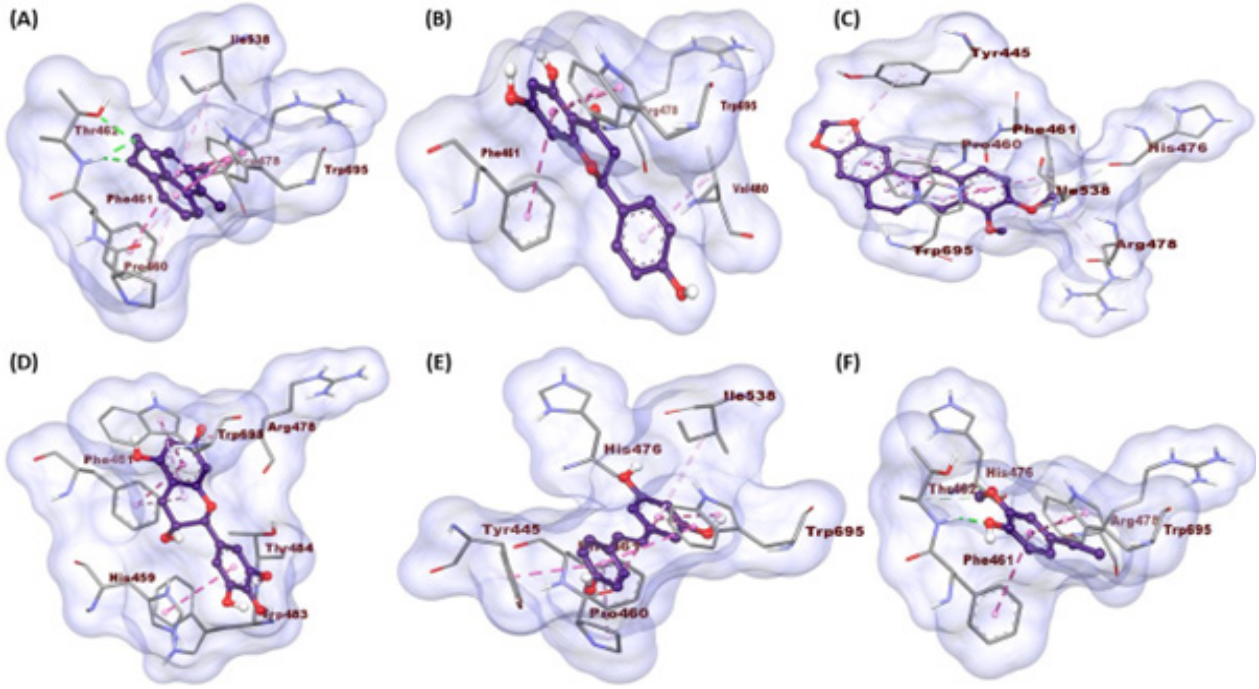

Figure 2: 3D poses and binding interactions of (A) Plumbagin, (B) Naringenin, (C) Berberine, (D) Epigallocatechin, (E) Resveratrol and (F) Apocynin with 5O0X.

His459 and donor-donor interactions with Arg478, Thr484 and Trp483 (Figure 2D). Resveterol was observed interacting through hydrogen bond with His476, through alkyl bonds with Ile538, Pro460 and via pi bonds with Phe461, Tyr445 and Trp695 (Figure 2E). Apocynin as a standard NOX inhibitor, interacted with His476, Thr462, and Arg478 by hydrogen bonding and with Phe461 and Trp695 by pi interactions (Figure 2F).

ADMET Assay

Extracted phytochemicals were gathered and examined for various physicochemical characteristics (Table 2) like Molecular Mass (MW), Hydrogen Bond Acceptors (HBA), Hydrogen Bond Donors (HBD), count of Rotatable Bonds (RB), partition coefficient (Log P), Molar Refractivity (MR), topological Polar

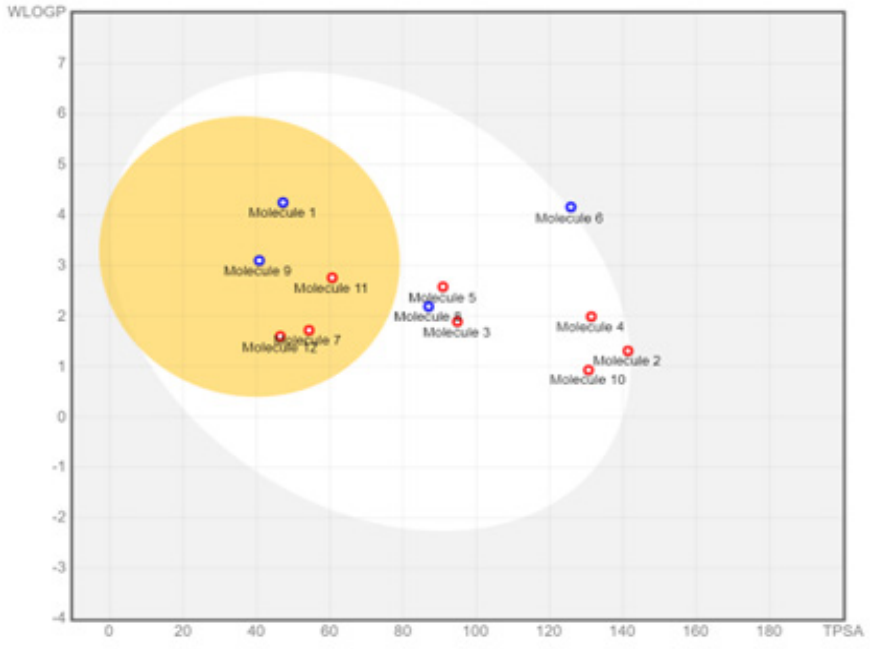

Figure 3: Hit molecules' boiled egg model created using SwissADME. The regions marked in yellow and lacking color represent the BBB and gastrointestinal tract, respectively. The presence of blue circles shows P-glycoprotein inhibition.

Table 2: Physicochemical properties of phytochemicals predicted using SwissADME to evaluate their drug likeliness.

Compounds	MW[a]	HBD[b]	HBA[c]	RB[d]	LogP[e]	AliLogS[f]	MR[g]	tPSA[h]
Tanshinone IIa	294.34	0	3	0	4.24792	-5.04	84.7	47.28
Ellagic acid	302.19	4	8	0	1.3128	-3.66	75.31	141.34
Emodin	270.24	3	5	0	1.8872	-4.37	70.78	94.83
Quercetin	302.24	5	7	1	1.988	-3.91	78.03	131.36
Apigenin	270.24	3	5	1	2.5768	-4.59	73.99	90.9
Curcuminoid	394.38	0	6	8	4.37474	-6.72	113.35	125.78
Plumbagin	188.18	1	3	0	1.7175	-3.07	51.07	54.37
Naringenin	272.25	3	5	1	2.5099	-3.99	71.57	86.99
Berberine	336.36	0	4	2	3.0963	-4.16	94.87	40.8
Epigallocatechin	306.27	6	7	1	1.2517	-2.29	76.36	130.61
Resveratrol	228.24	3	3	2	2.9738	-4.07	67.88	60.69
Apocynin	166.17	1	3	2	1.6034	-1.06	45.15	46.53

[a]Molecular mass (≤500 Da), [b]Hydrogen bond donors (≤ 5), [c]Hydrogen bond acceptors (≤ 10), [d]Rotational bonds (≤ 10), [e]Partition coefficient in oil to water (≤ 5), [f]Aqueous solubility (≤ 0), [g]molar refractivity (≤ 155), and [h]topological polar surface area (≤ 150[2]).

Surface Area (tPSA), aqueous solubility (Ali log S) utilizing SwissADME and pkCSM. Each of the hits possesses adequate physicochemical properties to qualify as a potential drug candidate. Epigallocatechin surpasses the HBD atmos threshold. This can be managed using innovative and advanced methods in formulation development. Therefore, many of the findings could potentially become more effective drug molecules based on their physical and chemical characteristics seen in computer-based analysis.

Subsequently, we examined various criteria for assessing drug-likeness such as Rule of five, Veber's rule, Ghose rule, Egan's rule and Muegge's rule to verify drug-likeness of hit molecules, with the number of parameters breaching each rule illustrated. Based on Lipinski's rule, a molecule may be considered a promising drug candidate if it meets the criteria of HBD (≤ 5), HBA (≤ 10), MW (≤ 500 Da), RB (≤ 5) and LogP (≤ 5), (Lipinski, 2004; Lipinski *et al.*, 2012). Every compound, excluding epigallocatechin, has been recognized as possessing the required characteristics to be evaluated as antioxidant medications aimed

at NOX5. According to Veber's rule, a molecule should have a polar surface area lower than 140 A^{o2} to exhibit enhanced bioavailability orally (Veber *et al*., 2002). Ellagic acid was discovered to breach this regulation. All substances apart from ellagic acid met the criteria of oral bioavailability as per the Egan rule with the required log P (-1-6) and tPSA (0-132 A2) (Egan *et al*., 2000). Muegge's rule comprises various parameters including lipophilicity (XLOGP3, -2-5), MW (200-600), cyclic rings (≤ 7), tPSA (≤ 150), heteroatoms (> 1), carbon atoms (> 4), HBA (≤ 10), HBD (≤ 5) and RB (≤ 15) (Muegge *et al*., 2001). Plumbagin, Epigallocatechin, and Apocynin were discovered to breach one of these principles. Ghose rule gave the optimal criteria of MW (160-480 Da), MR (40-130), Log P (-0.4-5.6), and atoms (20-70) for suitable candidates as a drug molecule (Ghose *et al*., 1999) and all the identified compounds satisfy these recommended characteristics.

We also evaluated Absorption, Distribution, Metabolism, Excretion, Toxicity (ADMET) factors such as intestinal absorption, $CaCO_2$ cell permeability, free drug fraction, volume of distribution (Vd), inhibition of P-glycoprotein substrates, and CYP2D6 and CYP3A4 enzymes for hits. All compounds except quercetin have satisfied the criteria of $CaCO_2$ cell permeability. Every hit showed adequate absorption in the human intestine, demonstrating improved oral bioavailability. The majority of the successful molecules met the requirements for volume of distribution and blocking of P-glycoprotein and CYP3A4 enzyme. No compound was obtained that blocks CYP2D6 enzyme.

Moreover, we evaluated the metabolism, elimination, and toxicity profiles of phytoconstituents. Most molecules exhibit moderate renal clearance, whereas berberine shows high clearance and naringenin shows low clearance. Berberine was identified as a substrate for the transporter responsible for the renal uptake in the OCT2 (proximal convoluted tubule). All identified compounds were found to be safe after assessment for cytotoxicity (hERG cell line), hepatotoxicity (except for curcuminoid), dermal toxicity (skin sensitization), and predictions for oral rat acute and oral rat chronic toxicity (LD_{50}, LOAEL respectively). Consequently, selected compounds might be utilized as potent drugs for targeting NOX5 as antioxidants in the future

We employed the BOILED-Egg method to predict the permeability of molecules through the Blood-Brain Barrier (BBB) and Gastrointestinal (GI) tract (Daina *et al*., 2016). The boiled egg model showed that the selected compounds had adequate absorption in GI and also inhibited the P-glycoprotein, a protein that plays a role in drug efflux from cells and BBB permeability (Figure 3).

MD Simulations

Molecular Dynamics (MD) simulations help to improve our understanding of the stability of phytoconstituents post binding with enzymes by analyzing various statistical parameters (Ghose *et al*., 1999). Following a comparable method, the successful element Tanshinone IIa, derived from docking score assessment, was put through MD simulations with GROMACS 2020.1 at different time points, reaching up to 50 ns.

The Tanshinone IIa-5O0X complex was subjected to MD simulation, and Figure 4 shows the graphical depiction of statistical parameter plots. The compound showed a Root Mean Square Deviation (RMSD) between 0.087-0.570 nm for the ligand and 0.0849-0.395 nm for the protein, averaging at 0.246 nm and 0.327 nm respectively (Figure 4A and 4B). This suggests a stable compound with minimal deviation at the active site. The RMSF value of this compound was found to be below 0.5 nm, suggesting minimal fluctuation of the ligand (Figure 4C). The RoG plot between 1.919-1.996 nm, having an average of 1.953 nm (Figure 4D), illustrates the compactness. The water molecules present in the active site of protein were able to reach a surface area ranging from 140.491-150.906 nm^2, having average of 146.384 nm^2 being observed (Figure 4E). The graph showing the number of hydrogen bonds formed over time indicates that Tanshinone IIa formed a maximum of three hydrogen bonds with 5O0X within 50 ns, while one hydrogen bond was constantly observed during entire period of 50 ns described in the Figure 4F.

NBT Assay

In vitro analysis was conducted on PC3 cell line to assess the NOX inhibitory activity of selected phytoconstituents via NBT assay. NOX inhibitory activity in terms of IC_{50} concentrations (nM) of selected molecules have been reported in Table 3.

Tanshinone IIa, Emodin, Quercetin, Curcuminoids, Plumbagin, Berberine, Epigallocatechin, and Resveratrol have been shown to have an IC_{50} value between 1-190 nM, demonstrating a strong inhibitory effect at low concentrations. Although Naringenin has an IC_{50} of 2 µM, a greater concentration is needed compared to other molecules to achieve the same level of inhibition. Regrettably, the lack of dose-dependent effect made it impossible to detect inhibition by Apocynin and Apigenin.

Cytochrome C Reductase Assay

In this assay, Tanshinone IIa, Quercetin, Curcuminoids, Berberine and Resveratrol showed IC_{50} values ranging from 13-538 nM, demonstrating effective NOX inhibition. Other molecules did not exhibit inhibition dependent on the dose (Table 4). Additionally, ellagic acid was eliminated from the *in vitro* study due to its poor solubility.

DISCUSSION

The results underscore the promise of phytoconstituents as inhibitors of NOX5. Of the compounds evaluated, Tanshinone IIa showed the strongest binding affinity and stability throughout MD simulations. Quercetin, Curcuminoids, and Resveratrol showed

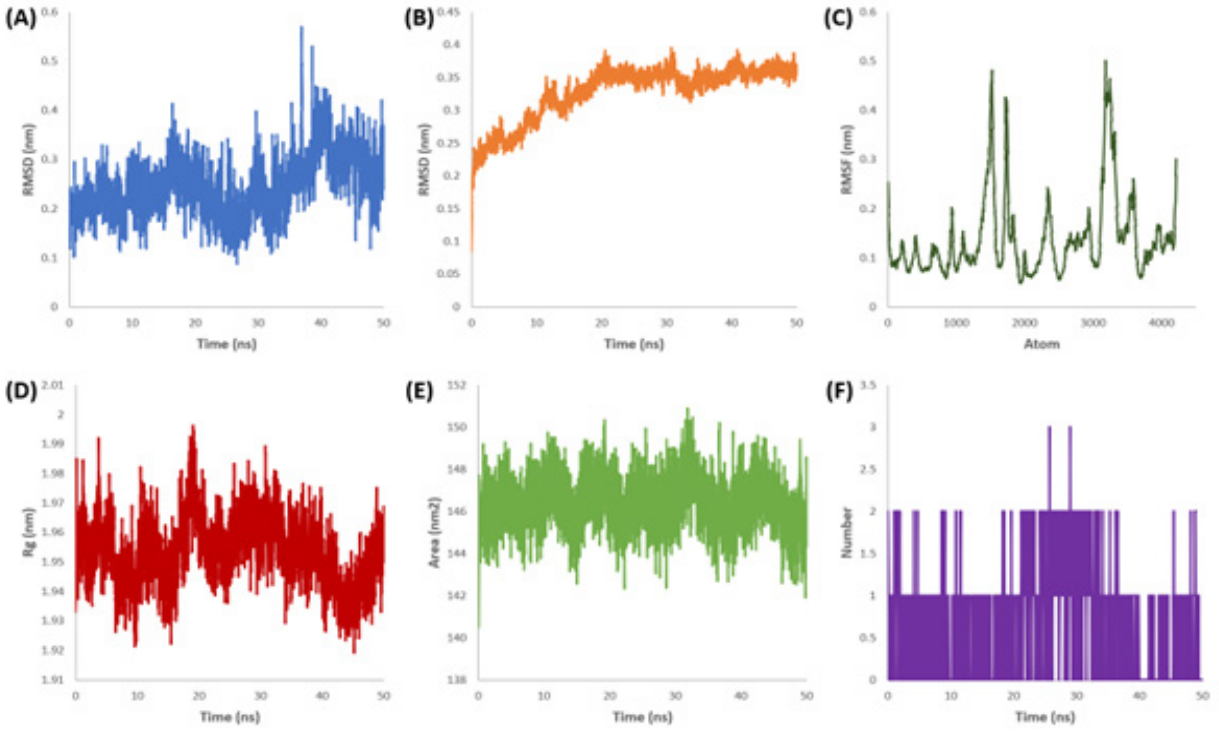

Figure 4: The graphs of (A) RMSD-Tanshinone IIa, (B) RMSD-protein, (C) RMSF-Tanshinone IIa, (D) RoG, (E) SASA, (F) hydrogen bonds for the 5O0X-Tanshinone IIa complex.

Table 3: Obtained IC_{50} (nM) values of selected phytoconstituents in NBT assay.

Phytoconstituents	IC_{50} (nM)
Tanshinone IIa	3.885
Emodin	24.655
Quercetin	1.059
Curcuminoids	173.452
Plumbagin	8.897
Naringenin	2017.920
Berberine	189.541
Epigallocatechin	3.943
Resveratrol	18.632
Apocynin	not detectable*
Apigenin	not detectable*

* % inhibition of NOX enzyme increased as the doses of the drugs decreased. Hence, IC_{50} value could not be determined.

Table 4: Obtained IC_{50} (nM) values of selected phytoconstituents in Cytochrome C Reductase assay.

Phytoconstituents	IC_{50} (nM)
Tanshinone IIa	141.977
Quercetin	261.607
Curcuminoids	113.052
Berberine	537.810
Resveratrol	13.724
Apocynin	89.792
Emodin	not detectable*
Apigenin	not detectable*
Plumbagin	not detectable*
Naringenin	not detectable*
Epigallocatechin	not detectable*

* % inhibition of NOX enzyme increased as the doses of the drugs decreased. Hence, IC_{50} value could not be determined.

encouraging pharmacokinetic and inhibitory characteristics as well.

The *in silico* findings correlated effectively with the *in vitro* tests, as the leading compounds significantly decreased ROS production through NOX5 inhibition. The ADMET evaluation also reinforced their drug-like properties, suggesting effective absorption and metabolic stability.

Although the majority of compounds conformed to drug-likeness standards, a few showed restrictions. The significant number of hydrogen bond donors in Epigallocatechin might influence its permeability, while the elevated topological polar surface area of Ellagic acid may affect its oral bioavailability. Nonetheless, these constraints could be alleviated by employing formulation strategies.

In summary, this research indicates that certain phytoconstituents, especially Tanshinone IIa, may serve as NOX5 inhibitors for future drug development and therapeutic uses.

CONCLUSION

According to *in silico* and *in vitro* research, Tanshinone IIa, Quercetin, Curcuminoids, Berberine, and Resveratrol have shown effective NOX inhibitory levels and favourable pharmacokinetic profiles and drug-likeliness. Therefore, they could serve as promising herbal drug candidates as inhibitors of NOX5, which should be incorporated for further studies in future.

ABBREVIATIONS

ADMET: Absorption, Distribution, Metabolism, Excretion, and Toxicity; **BBB:** Blood-Brain Barrier; **CGenFF:** CHARMM General Force Field; **CHARMM:** Chemistry at Harvard Macromolecular Mechanics; **DMSO:** Dimethyl Sulfoxide; **DUOX:** Dual Oxidase; **FAD:** Flavin Adenine Dinucleotide; **HBA:** Hydrogen Bond Acceptors; **HBD:** Hydrogen Bond Donors; **LogP:** Partition Coefficient (Oil to Water); **LOAEL:** Lowest Observed Adverse Effect Level; **MD:** Molecular Dynamics; **MW:** Molecular Weight; **NBT:** Nitroblue Tetrazolium; **NADPH:** Nicotinamide Adenine Dinucleotide Phosphate; **NOX:** NADPH Oxidases; **PC3:** Prostate Cancer Cell Line 3; **PDB:** Protein Data Bank; **P-gp:** P-glycoprotein; **PK:** Pharmacokinetics; **RMSD:** Root Mean Square Deviation; **RMSF:** Root Mean Square Fluctuation; **RB:** Rotational Bonds; **RoG:** Radius of Gyration; **ROS:** Reactive Oxygen Species; **SASA:** Solvent Accessible Surface Area; **tPSA:** Topological Polar Surface Area; **VDss:** Volume of Distribution at Steady State.

CONFLICT OF INTEREST

The authors declare that there is no conflict of interest.

REFERENCES

Abliz, A., Chen, C., Deng, W., Wang, W., & Sun, R. (2016). NADPH oxidase inhibitor apocynin attenuates PCB153-induced thyroid injury in rats. International Journal of Endocrinology, 2016, Article 8354745. https://doi.org/10.1155/2016/8354745

Abraham, M. J., Hess, B., & Lindahl, E. (n.d.). D. van der S. GROMACS. Zenodo, 2020(1), (Article 2020. 1). https://doi.org/10.5281/zenodo.4054996

Abraham, M. J., Murtola, T., Schulz, R., Páll, S., Smith, J. C., Hess, B., & Lindahl, E. (2015). Gromacs: High performance molecular simulations through multi-level parallelism from laptops to supercomputers. SoftwareX, 1–2, 19–25. https://doi.org/10.1016/j.softx.2015.06.001

Agnes, J., Yun, G., Susan, M., Alice, C., Linda, M., Josephus, V. B., Krishnendu, R., James, H., & DOROSHOW. (2009). Expression of NADPH oxidase homologues and accessory genes in human cancer cell lines, tumours and adjacent normal tissues. Free Radical Research, 43(6), 523–532. https://doi.org/10.1080/10715760902918683.Expression

Altenhöfer, S., Radermacher, K. A., Kleikers, P. W. M., Wingler, K., & Schmidt, H. H. H. W. (2015). Evolution of NADPH oxidase inhibitors: Selectivity and mechanisms for target engagement. Antioxidants and Redox Signaling, 23(5), 406–427. https://doi.org/10.1089/ars.2013.5814

Bedard, K., Jaquet, V., & Krause, K.-H. (2012). NOX5: From basic biology to signaling and disease. Free Radical Biology and Medicine, 52(4), 725–734. https://doi.org/10.1016/j.freeradbiomed.2011.11.023

Choi, H. S., Kim, J. W., Cha, Y.-N., & Kim, C. (2006). A quantitative nitroblue tetrazolium assay for determining intracellular superoxide anion production in phagocytic cells. Journal of Immunoassay and Immunochemistry, 27(1), 31–44. https://doi.org/10.1080/15321810500403722

Cipriano, A., Viviano, M., Feoli, A., Milite, C., Sarno, G., Castellano, S., & Sbardella, G. (2023). NADPH oxidases: From molecular mechanisms to current inhibitors. Journal of Medicinal Chemistry, 66(17), 11632–11655. https://doi.org/10.1021/acs.jmedchem.3c00770

Daina, A., Michielin, O., & Zoete, V. (2017). SwissADME: A free web tool to evaluate pharmacokinetics, drug-likeness and medicinal chemistry friendliness of small molecules. Scientific Reports, 7, Article 42717. https://doi.org/10.1038/srep42717

Daina, A., & Zoete, V. (2016). A BOILED-egg to predict gastrointestinal absorption and brain penetration of small molecules. ChemMedChem, 11(11), 1117–1121. https://doi.org/10.1002/cmdc.201600182

Dassault systèmes BIOVIA, Discovery Studio modeling environment (release 2021). Dassault Systèmes. (2020). (n.d.).

Egan, W. J., Merz, K. M., & Baldwin, J. J. (2000). Prediction of drug absorption using multivariate statistics. Journal of Medicinal Chemistry, 43(21), 3867–3877. https://doi.org/10.1021/jm000292e

Ghose, A. K., Viswanadhan, V. N., & Wendoloski, J. J. (1999). A knowledge-based approach in designing combinatorial or medicinal chemistry libraries for drug discovery. 1. A qualitative and quantitative characterization of known drug databases. Journal of Combinatorial Chemistry, 1(1), 55–68. https://doi.org/10.1021/cc9800071

Huang, J., Rauscher, S., Nawrocki, G., Ran, T., Feig, M., de Groot, B. L., Grubmüller, H., & MacKerell, A. D. (2017). CHARMM36: An improved force field for folded and intrinsically disordered proteins. Biophysical Journal, 112(3), 175a–176a. https://doi.org/10.1016/j.bpj.2016.11.971

Kumar Tiwari, A., Gandhi, V., Agarwal, S., Tyagi, V., Agarwal, V., Jindal, D., Rachana, R., & Singh, M. (2023). In silico validation of apocynine and NADPH Oxidase (NOX) enzyme for inhibiting ROS injuries. Materials Today: Proceedings, 80(xxxx), 2375–2377. https://doi.org/10.1016/j.matpr.2021.06.361

Lipinski, C. A. (2004). Lead- and drug-like compounds: The rule-of-five revolution. Drug Discovery Today. Technologies, 1(4), 337–341. https://doi.org/10.1016/j.ddtec.2004.11.007

Lipinski, C. A., Lombardo, F., Dominy, B. W., & Feeney, P. J. (2012). Experimental and computational approaches to estimate solubility and permeability in drug discovery and development settings. Advanced Drug Delivery Reviews, 64, 4–17.

Magnani, F., Nenci, S., Millana Fananas, E. M., Ceccon, M., Romero, E., Fraaije, M. W., & Mattevi, A. (2017). Crystal structures and atomic model of NADPH oxidase. Proceedings of the National Academy of Sciences of the United States of America, 114(26), 6764–6769. https://doi.org/10.1073/pnas.1702293114

Morris, G. M., Huey, R., Lindstrom, W., Sanner, M. F., Belew, R. K., Goodsell, D. S., & Olson, A. J. (2009). AutoDock4 and AutoDockTools4: Automated docking with selective receptor flexibility. Journal of Computational Chemistry, 30(16), 2785–2791. https://doi.org/10.1002/jcc.21256

Muegge, I., Heald, S. L., & Brittelli, D. (2001). Simple selection criteria for drug-like chemical matter. Journal of Medicinal Chemistry, 44(12), 1841–1846. https://doi.org/10.1021/jm015507e

O'Boyle, N. M., Banck, M., James, C. A., Morley, C., Vandermeersch, T., & Hutchison, G. R. (2011). Open Babel: An Open chemical toolbox. Journal of Cheminformatics, 3(10), 33. https://doi.org/10.1186/1758-2946-3-33

Pires, D. E. V., Blundell, T. L., & Ascher, D. B. (2015). pkCSM: Predicting small-molecule pharmacokinetic and toxicity properties using graph-based signatures. Journal of Medicinal Chemistry, 58(9), 4066–4072. https://doi.org/10.1021/acs.jmedchem.5b00104

Pizzino, G., Irrera, N., Cucinotta, M., Pallio, G., Mannino, F., Arcoraci, V., Squadrito, F., Altavilla, D., & Bitto, A. (2017). Oxidative stress: Harms and benefits for human health. Oxidative Medicine and Cellular Longevity, 2017, Article 8416763. https://doi.org/10.1155/2017/8416763

pkCSM: Pharmacokinetic properties. (n.d.). http://biosig.unimelb.edu.au/pkcsm/prediction

Protein Data Bank. (n.d.). https://www.rcsb.org/

PubChem. (n.d.). https://pubchem.ncbi.nlm.nih.gov/

Silveira, C. M., Besson, S., Moura, I., Moura, J. J. G., & Almeida, M. G. (2010). Measuring the cytochrome c nitrite reductase activitypractical considerations on the enzyme assays. Bioinorganic Chemistry and Applications, 2010, Article 634597. https://doi.org/10.1155/2010/634597

Steffen, C., Thomas, K., Huniar, U., Hellweg, A., Rubner, O., & Schroer, A. (2010). Software news and updates TmoleX-a graphical user interface for TURBOMOLE. Journal of Computational Chemistry, 31(16), 2967–2970. https://doi.org/10.1002/jcc.21576

Vanommeslaeghe, K., Acharya, C., Kundu, S., Zhong, S., Shim, J., Darian, E., Guvench, O., Lopes, P., & Vorobyov, I. MA J. (2009). CHARMM general force field: A force field for drug-like molecules compatible with the CHARMM ALL-atom additive biological force fields. Journal of Computational Chemistry, 31, 671–690.

Veber, D. F., Johnson, S. R., Cheng, H.-Y., Smith, B. R., Ward, K. W., & Kopple, K. D. (2002). Molecular properties that influence the oral bioavailability of drug candidates. Journal of Medicinal Chemistry, 45(12), 2615–2623. https://doi.org/10.1021/jm020017n

Vermot, A., Petit-Härtlein, I., Smith, S. M. E., & Fieschi, F. (2021). NADPH oxidases (Nox): An overview from discovery, molecular mechanisms to physiology and pathology. Antioxidants, 10(6), Article 890. https://doi.org/10.3390/antiox10060890

Whitehouse, S., Chen, P.-L., Greenshields, A. L., Nightingale, M., Hoskin, D. W., & Bedard, K. (2016). Resveratrol, piperine and apigenin differ in their NADPH-oxidase inhibitory and reactive oxygen species-scavenging properties. Phytomedicine, 23(12), 1494–1503. https://doi.org/10.1016/j.phymed.2016.08.011

Yu, W., He, X., Vanommeslaeghe, K., & MacKerell, A. D. (2012). Extension of the CHARMM general force field to sulfonyl-containing compounds and its utility in biomolecular simulations. Journal of Computational Chemistry, 33(31), 2451–2468. https://doi.org/10.1002/jcc.23067

Cite this article: Shah P, Shah G. *In silico* and *in vitro* Evaluation of Phytoconstituents for their NOX5 Inhibitory Activity. Int. J. Pharm. Investigation. 2026;16(1):133-142.